EPiC Series in Built Environment

Volume 7, 2026, Pages 733–742

Proceedings of Associated Schools of Construction 62nd Annual International Conference

Automated Construction Site Intrusion Deterrence Through 2D LiDAR and Passive Infrared Sensing

Caleb M. Powell[1], Eric M. Wetzel[1], and Kenneth S. Sands II[1]
[1]Auburn University

Construction sites require effective security monitoring during non-operational hours to prevent theft, vandalism, and safety concerns. However, construction site security is often overlooked and limited to fencing and signage systems. Staffed security and multi-camera setups are vulnerable to human-error and often require continual adjustment over the life of a project, and many commercially available autonomous systems remain financially expensive. This research aims to develop and evaluate a low-cost, autonomous, moveable monitoring system that integrates 2D Light Detection and Ranging (LiDAR) and Passive Infrared (PIR) sensors to detect motion, identify unauthorized activity, and deter intrusions on construction sites. Experimental testing evaluated detection reliability, false alarm rates, and environmental performance in indoor and outdoor settings. Results showed that LiDAR was able to accurately detect motion with ranges exceeding 30 feet and demonstrated reliability in varying environmental conditions. PIR sensors did not demonstrate reliable motion detection, and additional research is needed to improve their performance in construction settings. These results demonstrate that combining LiDAR and PIR sensing offers a practical basis for affordable, autonomous construction site security. Future work will address PIR calibration, environmental hardening, and algorithm parameter tuning.

Keywords: Construction Jobsite, Security, Automation, LiDAR, PIR

Introduction

Construction sites are susceptible to intrusion and theft due to the natural curiosity they invoke combined with their general vacancy in the late evening and weekends. Unauthorized access to construction sites introduces significant safety concerns, as these intruders are particularly vulnerable to site hazards, while theft remains a major financial burden to construction companies. A study of 102 contractors in the Southeastern United States conducted in 2005 estimated that the cost of theft and vandalism totals $1,682 per $1 million of self-performed work (Berg et al., 2005). Most of the theft took place on sites where equipment was left unattended during non-operational hours and limited security measures were present. In 2016, the National Equipment Register (NER) and the National Insurance Crime Bureau (NICB) released a report estimating an annual loss of $400 million dollars in equipment theft across all domains, highlighting poor equipment and site security as contributing factor (Verisk Crime Analytics, Inc., 2017). This report suggests that equipment theft is an ongoing and prevalent issue in the construction industry. In 2019, a meta-analysis of 15,000 incidents from the National Incident-Based Reporting System (NIBRS) revealed that recovery rates for stolen construction items were alarmingly low - less than 7% - with contractors losing an average of $6,000 per theft incident (Shrestha et al., 2019). While these figures are staggering, the true cost of

construction theft is likely much higher due to underreporting, induced schedule delays, and increased insurance premiums. Despite this, there is limited research on construction site theft and prevention techniques (Boba et al., 2008).

Related Work

Unfortunately, research efforts in job site security are very limited and most sites only use standard security measures such as lockboxes, fences, and warning signage (Berg et al., 2005 & Boba et al., 2008). Some sites deploy more sophisticated measures such as pan-tilt-zoom camera (Sentry Pods, 2025), but manual monitoring can be time consuming, prone to human error, and may require consistent camera adjustments as the project evolves. AI-powered camera systems such as SimpliSafe (2025) and Ring (2025) exist; however, the construction industry has been slow to adopt these strategies, likely due to cost and limited case studies (Musarat et al., 2024 & Ojha et al. 2022). However, autonomous monitoring of construction sites has shown to reduce fatigue and time consumption drastically (Musarat et al., 2024).

Therefore, this research focuses on the development and evaluation of a cost-effective, autonomous system for detecting and deterring intrusions on construction job sites. The novelty of the system lies in three key aspects. First, it repurposes an inexpensive 2D hobby-grade LiDAR sensor - typically used in robotics - for security monitoring. While 2D LiDAR pucks are commonly employed for navigation and obstacle detection in mobile platforms, this study leverages their spatial measurement capabilities to monitor defined zones for unauthorized movement, offering a low-cost alternative to traditional surveillance systems. The second is the mobile nature of the device - placed on a tripod, requiring only an extension cord for power, the system can be placed in locations with sensitive materials and equipment and then moved when those items are no longer at risk for theft. Finally, the system operates independent of wireless networking. Most construction projects have areas of poor or absent Wi-Fi signal, especially as the project evolves. In lieu of requiring multiple access points and adjusting those as the structure is erected, this system focuses on deterrence, eliminating the need for network connectivity.

System Design

The system is intended to be deployed during non-operational hours and continuously monitors its surroundings for motion using a combination of sensors. When motion is detected, two cameras will begin recording for a set duration, and a speaker will emit an alarm sound. Once the allotted time has surpassed for the video and alarm, the system resets, and resumes monitoring. The recorded video is stored internally as documentation for the system administrator, while the alarm serves as a deterrent for the potential trespasser. Figure 1 depicts the system inside of a 3D printed housing mounted to a camera tripod.

Figure 1. Images of System Hardware

Hardware

The hardware was selected to align with the design goals of cost-effectiveness. For motion detection, the system utilizes a combination of Light Detection and Ranging (LiDAR) and PIR (Passive Infrared) sensors. LiDAR provides precise, detailed, and consistent measurements at high speed and long range. Many LiDAR units are limited to two-dimensional measurements (radial distance, and angle) on a single vertical plane. To address this limitation, two PIR sensors were added to the system on adjacent sides of the housing. PIR sensors are inexpensive, consume minimal power, and detect changes in thermal energy in a wide field of view (FOV), enabling motion detection above and below the vertical plane monitored by LiDAR. The system's PIR sensor has a shorter maximum detection range (7 meters) than its LiDAR sensor (12 meters) and measures only binary motion data in a 120-degree FOV.

For computational hardware, a Raspberry Pi 5 (RPi 5) was selected primarily for its power efficiency and two 4-lane MIPI CSI ports allowing direct communication with two Raspberry Pi Camera Modules via the picamera2 python library. The two camera modules were mounted to the housing above the PIR sensors. For audio output, a generic USB speaker was selected over Bluetooth to increase system reliability. Table 1 is a summary of all hardware used and their approximate costs.

Table 1. System Hardware Summary

Component	**Description**	**Cost**
LiDAR	Slamtec RPLidar A1M8	$100
PIR x2	Adafruit Passive Infrared Sensor	$20
CPU	Raspberry Pi 5	$100
Camera x2	Raspberry Pi Camera Module 2	$60
Speaker	Generic USB Speaker	$15
Tripod	-	$30
Total	-	**$325**

Software

Motion detection using PIR sensors is as straightforward as reading a binary signal from the RPi 5's GPIO header. The sensor outputs a high signal (voltage) when motion is detected, and a low signal (0V) when the area around the sensor is static. LiDAR motion detection is far more complicated and results in several system limitations that will be discussed in more detail in the discussion section of this paper. This section will summarize the algorithm design to facilitate the discussion.

To perform motion detection with LiDAR we must first identify a set of polar coordinates that define what a scan of the environment should look like when it is undisturbed. We call this set of polar coordinates the *baseline* scan. A baseline can be determined by performing numerous scans of an undisturbed environment and assigning an expected distance value r_i for every possible angle value θ_i in a scan. After a baseline is determined, subsequent scans of the environment can be compared to it to detect motion. For example: if angle θ_i has a baseline distance value of r_i and subsequent scans show that angle θ_i is now reading a distance value $\ll r_i$, the environment likely has been disturbed. This allows the system to both identify and locate motion within the environment.

Binning

A single LiDAR scan can produce thousands of data points. Performing multiple stationary scans of an environment does not consistently produce identical data points due to error in measurement (noise). This makes determining the expected distance value for every angle challenging. To address this, the system first divides the angular data into discrete intervals. All data points within each

interval are assigned the same angular value. This process is known as *binning* and produces sets of discrete angular range values known as *bins*. The span (or amount) of continuous angular values $[\theta_{start}, \theta_{end})$ assigned to the same bin are called the *bin width*. For example: If the bin width is 5°, all angles in the continuous range *(0°, 5°]* map to bin *0°*, and all angles in *(5°, 10°]* are mapped to bin *5°*. This process maps the continuous angular domain of scan data into discrete angular quantities.

K-Means Clustering

To create a baseline, each discrete angular bin must be assigned an expected distance value. Motion is determined when a subsequent scan produces a distance in any bin that is shorter than the baseline. The initial approach was to define the expected distance in each bin as the minimum distance measured in that bin across all scans in the baseline. However, the LiDAR used in the system operates in the near-infrared spectrum and is highly susceptible to interference from surrounding light. This produces occasional outlier measurements that are much closer to the system's origin. If left unfiltered, these anomalies would distort the system's perception of its environment by establishing a baseline measurement that is disconnected from the true spatial map. Increasing the number of scans in the baseline can mitigate this but also allows for additional interference to bias the baseline closer towards the system's origin.

To address these issues, a k = 2 means clustering algorithm is applied to the distance values in each bin under the assumption that the data consists of two clusters: one representing consistent distance measure from true static objects in the environment and a second representing outlier measurements induced by sensor interference. This assumption provides a computationally inexpensive means for isolating possible anomalous distance readings and can be easily implemented using the scikit-learn python library.

When one cluster contains more than 80% of the data, the assumption is considered valid. The baseline for the bin is then defined as the minimum distance measured within that cluster, and the remaining cluster is treated as an outlier. If no cluster holds more than 80% of data, the assumption is considered invalid, and the baseline is defined as the minimum distance measured in the entire bin. Figure 2 illustrates the result of k-means clustering applied to a single bin of data collected from 2,000 scans. The color of each bar corresponds to the cluster assignment produced by the k-means algorithm. Since Cluster 0 contains 92.4% of the total data, the baseline for this bin was established at the minimum value within Cluster 0, shown as the dashed red vertical line.

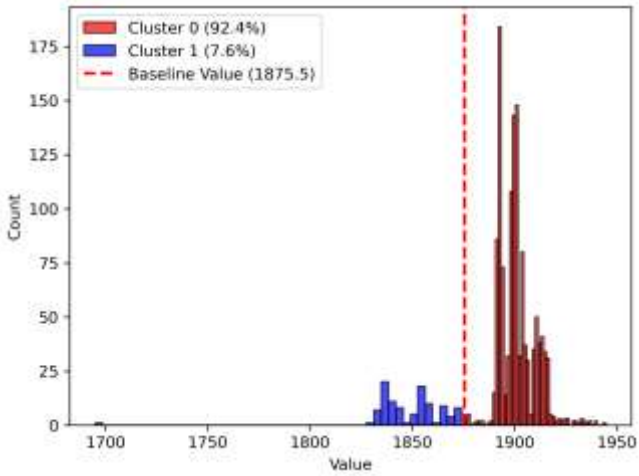

Figure 2: K-Means clustering identifying baseline scan outliers

Repeat Frames

K-means clustering reduces the outlier's influence on the baseline but does not remove outliers from subsequent scans. To keep the system from falsely identifying outlier data as motion in the environment- activating the deterrence system - motion is only determined to be valid if the distance measured in each bin remains shorter than its baseline value for multiple consecutive scans. The number of scans was set to 11, which is approximately 2 seconds given that the system's LiDAR operates at a rotational speed of 5.5Hz.

Experimental Design

Experiments were conducted in indoors and outside spaces of Miller M. Gorrie Center at Auburn University. Testing was done in both indoor and outdoor environments to simulate construction sites at varying stages of development. The system was placed in a fixed location, and radial distances extending to 60 feet were marked on the floor at 10-foot increments along the LiDAR's zero-degree axis. Figure 3 depicts the two experimental setups.

Figure 3. Experimental setup for indoor and outdoor environments

The goal of this experiment was to measure the responsiveness and accuracy of the system and determine if changes in environmental conditions had an influence. Responsiveness is defined as how quickly the system detects motion after a participant has entered the scanning range. Accuracy is defined by the frequency of false positive motion detection. Motion detection using the LiDAR and PIR sensors were tested independently to assess their respective capabilities and limitations.

LiDAR Experimentation

For the LiDAR experimentation, a baseline was established for both environments using 100 scans, as described in the software design. Figure 4 shows the baseline and scan data from the indoor environment, where radial distances are measured in millimeters.

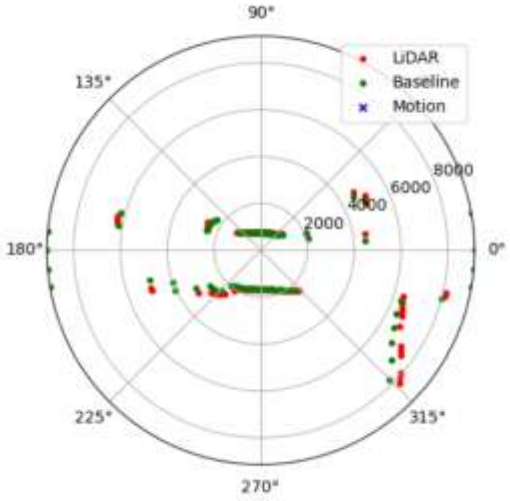

Figure 4. Indoor experimental baseline

Two walking styles were evaluated at each distance increment:

1. Normal walking speed with a natural gait
2. Extremely slow walking speed with a very short gate (creeping)

During the first trial, the maximum LiDAR scanning distance was set to 10 feet. Beginning at the 60-foot mark, the participant walked towards the system using the first walking style and stopped when the system detected motion. The radial distance between the participant and the system was measured and recorded by the LiDAR sensor. This process was repeated for five trials, and then the recorded distances were averaged and converted from millimeters to feet. The process was then repeated using the second walking style. Once data was collected for both walking styles, the maximum LiDAR range was increased by 10 feet, and data collection for the subsequent set of trials began. This process was repeated until motion detection was no longer successful.

PIR Experimentation

Experimentation for the PIR sensor was conducted in a similar fashion. However, only binary motion data can be collected, and detection ranges cannot be easily controlled. The sensitivity and fire rate of the sensor can be adjusted using two potentiometers, but doing so is inconvenient to the end user and difficult to measure accurately in experimentation. As a result, the potentiometers were left in their factory positions, and maximum scanning distances were not controlled during experimentation. Figure 6 illustrates a flow diagram of the experimental design used to independently evaluate the effects of environment, walking style, and sensor choice on motion detection performance.

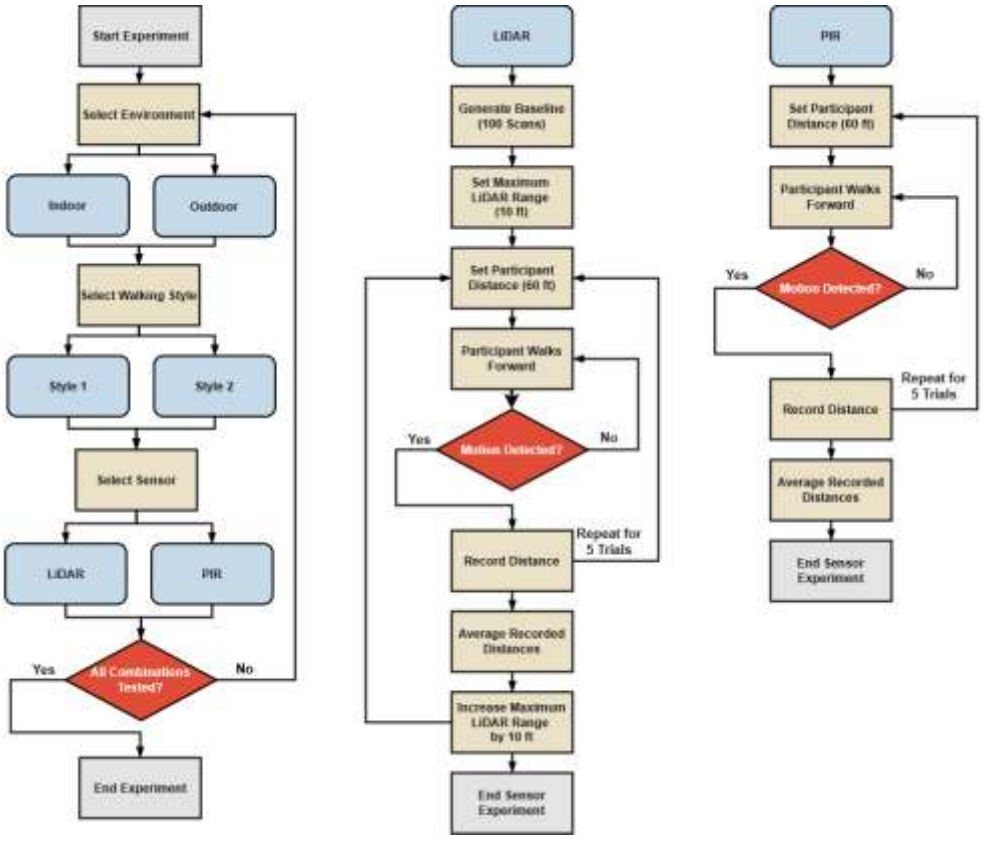

Figure 6. Flow diagram of Experimental Design

Results and Analysis

LiDAR Results

Results of indoor testing indicate that LiDAR motion detection was very accurate and responsive. Table 2 summarizes the average distance the LiDAR sensor measured the participant at when motion was detected during each trial. The participant was able to walk further past the maximum scanning threshold when using walking style one when compared to walking style two. For scanning ranges ≤ 30 feet, the difference (or delta) between detection distances of both walking styles averaged approximately 2 feet. However, at ranges ≥ 30 feet, the difference between walking styles increased to approximately 8 feet. At scanning ranges ≥ 40 feet, the system failed to detect motion until the participant was near or beyond the 40-foot mark. As a result, motion detection was considered unsuccessful at ranges ≥40 feet. During data collection, the system made 5 false-positive motion detections each in the 325° bin at distances of 23 feet.

Table 2. Averaged Results from Indoor Testing

Walking Style	10 FT	20 FT	30 FT	40 FT	60 FT
1	6.21	17.50	26.62	31.51	30.60
2	8.34	18.99	28.50	38.41	39.52
Delta	2.14	1.49	1.88	6.90	8.92

Outdoor testing produced results consistent with indoor testing. Table 3 shows the average detection distances recorded for each trial. Motion detection for walking style 2 was shown to be more responsive than walking style 1. The average detection delta for the two walking styles was approximately 2 feet when detection ranges were ≤ 30 feet but increased substantially for detection ranges ≥ 30 feet. No false positives were detected during outdoor testing.

Table 3. Averaged Results from Outdoor Testing

Walking Style	10 FT	20 FT	30 FT	40 FT	60 FT
1	7.35	15.81	26.31	27.28	28.08
2	9.08	18.55	28.59	35.13	41.65
Delta	1.73	2.74	2.28	7.84	13.56

Table 4 shows the delta with constant walking style, but varying environment. For walking style 1, changes in environmental conditions resulted in an average delta of 1.05 feet at ranges ≤ 30 feet. At ranged ≥30 feet, the delta increased to 3.38 feet. For walking style 2, the delta was slightly smaller with an average value of 0.42 feet for ranges ≤ 30 feet and 2.71 feet for ranges ≥ 30 feet. These results indicate that changes in environmental conditions have a greater impact on walking style 1 than walking style 2.

Table 4. Delta Between Indoor and Outdoor Averaged Testing

Walking Style	10 FT	20 FT	30 FT	40 FT	60 FT
1	1.14	1.69	0.31	4.23	2.52
2	0.74	0.44	0.09	3.29	2.13

Overall, detection performance using walking style two was significantly more responsive. This is likely attributed to the system requirement of detecting motion for 11 consecutive frames. Given that an average person walks approximately 3-4 feet per second, and 11 scans corresponds to roughly 2 seconds, a delta of 2-8 ft is consistent with expected system performance.

PIR Results

The PIR sensor made a large number false-positive detections during testing. Test data for PIR sensors was excluded since isolating the exact cause of the false positives was difficult and the frequency of their occurrence made identifying true positives challenging. The most likely cause is interference from surrounding light.

Discussion

K-Means Clustering and Indoor Testing

Indoor LiDAR testing produced five false positive detections. Although infrequent, they all detected motion in identical regions. This region corresponds to the two walkway openings toward the front-right side of the systems. This issue is likely a result of the binning and k-means clustering described in the software design section. When clustering was performed on this bin, several data points were likely collected from the nearest wall while the majority were collected from wall just beyond the opening. This would result in the closer wall being labeled as outlier data. However, during subsequent scans the LiDAR could have consistently detected this wall. This behavior was not exhibited during outdoor testing.

Limitation of Weather Conditions

Initial outdoor testing was conducted under direct sunlight on a hot day. This resulted in data acquisition failure as the LiDAR unit exceeded its maximum operating temperature of 104° F. A second round of testing was performed in overcast conditions but was interrupted by rainfall since the system currently lacks any form of waterproofing.

Future Work

Future work could look at hardware solutions such as physical shielding from the direct sunlight, infrared filters, and adjustment to PIR sensitivity, while software solutions may include similar signal smoothing techniques that were used in the LiDAR data. In the hardware design, heat-sink and housing solutions are needed for resiliency to weather conditions. To reduce the false positive reads from the LiDAR, several potential methods could be tested: dynamic baseline monitoring, improved cluster algorithms (e.g. density-based methods), additional senor fusion (e.g. integrating the cameras), or a pre-baseline mapping scan for localization of known architectural features. Given that the system is intended to be deployed on unsecured sites, future work should investigate theft-protection measures to mitigate theft of the device itself, such as integrating an inertial measurement unit (IMU) for displacement detection and deploying a tamper-resistant enclosure. These improvements could allow the system to perform more accurately and reliably in a common construction site environment.

Conclusion

The development and analysis of this system demonstrate the capability of producing cost effective and systems towards autonomous construction site security. Although the PIR sensor performed unreliably, additional research into PIR applications for construction security can increase the performance of the system at minimal cost. The LiDAR sensor implementation performed very accurately at ranges ≤ 30 feet and demonstrated reliability in varying environmental conditions and walking styles.

Advancements in job site security can improve safety, productivity, and construction cost by minimizing unauthorized intrusions. Continued research in affordable autonomous security systems is essential to accelerate their adoption within the construction industry. This research serves as a steppingstone towards a safer and more efficient building process.

References

Berg, R., & Hinze, J. (2005). Theft and Vandalism on Construction Sites. Journal of Construction Engineering and Management, 131(7), 826–833. https://doi.org/10.1061/(ASCE)0733-9364(2005)131:7(826)

Boba, R., & Santos, R. (2008). A Review of the Research, Practice, and Evaluation of Construction Site Theft Occurrence and Prevention: Directions for Future Research. *Security Journal*, *21*(4), 246–263. https://doi.org/10.1057/palgrave.sj.8350063

Musarat, M. A., Khan, A. M., Alaloul, W. S., Blas, N., & Ayub, S. (2024). Automated monitoring innovations for efficient and safe construction practices. Results in Engineering, 22, 102057. https://doi.org/10.1016/j.rineng.2024.102057

Ojha, A., Habibnezhad, M., Jebelli, H., & Leicht, R. (2022). Barrier Analysis of Effective Implementation of Robotics in the Construction Industry. In Construction Research Congress 2022 (pp. 661–669). https://doi.org/doi:10.1061/9780784483961.069

Ring. (2025). Jobsite Security. https://ring.com/jobsite-security

SentryPods. (2025). SentryPods. https://sentrypods.com/
Shrestha, Joseph; and Osborne, Dustin Lee. 2019. An Exploratory Look at Thefts from Construction Sites. Annual Associated Schools of Construction International Conference, Denver, CO. https://dc.etsu.edu/etsu-works/5471/
SimpliSafe. (2025). Buisness Security Systems. https://simplisafe.com/business
Verisk Crime Analytics, Inc. (2017). 2016 equipment theft report. Verisk Crime Analytics, Inc. https://www.ner.net/wp-content/uploads/2017/10/Annual-Theft-Report-2016.pdf